4-1999

The structure and properties of methylenetetrahydrofolate reductase from *Escherichia coli* suggest how folate ameliorates human hyperhomocysteinemia

Brian D. Guenther
University of Michigan

Christal A. Sheppard
University of Nebraska-Lincoln, christalsheppard@unl.edu

Pamela Tran
McGill University

Rima Rozen
McGill University

Rowena G. Matthews
University of Michigan, rmatthew@umich.edu

See next page for additional authors

Published in *Nature Structural Biology* 6:4 (April 1999), pp. 359–365; doi: 10.1038/7594

Submitted November 13, 1998; accepted December 7, 1998

The structure and properties of methylenetetrahydrofolate reductase from *Escherichia coli* suggest how folate ameliorates human hyperhomocysteinemia

Brian D. Guenther,[1] Christal A. Sheppard,[2] Pamela Tran,[4] Rima Rozen,[4] Rowena G. Matthews,[1, 2, 3] and Martha L. Ludwig [1, 2, 3]

1. Biophysics Research Division, University of Michigan , Ann Arbor Michigan 48109-1055, USA
2. Program in Cellular and Molecular Biology, University of Michigan, Ann Arbor Michigan 48109-1055, USA
3. Department of Biological Chemistry, University of Michigan , Ann Arbor Michigan 48109-1055, USA
4. Departments of Human Genetics, Pediatrics and Biology, McGill University, Montreal Children's Hospital, Montreal, Canada H3H 1P3

Authors Guenther and Sheppard contributed equally to the research described in this paper.

Corresponding authors — M. L. Ludwig ludwig@biop.umich.edu or R. G. Matthews rmatthew@umich.edu

Abstract

Elevated plasma homocysteine levels are associated with increased risk for cardiovascular disease and neural tube defects in humans. Folate treatment decreases homocysteine levels and dramatically reduces the incidence of neural tube defects. The flavoprotein methylenetetrahydrofolate reductase (MTHFR) is a likely target for these actions of folate. The most common genetic cause of mildly elevated plasma homocysteine in humans is the MTHFR polymorphism A222V (base change C677→T). The X-ray analysis of *E. coli* MTHFR, reported here, provides a model for the catalytic domain that is shared by all MTHFRs. This domain is a $\beta_8\alpha_8$ barrel that binds FAD in a novel fashion. Ala 177, corresponding to Ala 222 in human MTHFR, is near the bottom of the barrel and distant from the FAD. The mutation A177V does not affect K_m or k_{cat} but instead increases the propensity for bacterial MTHFR to lose its essential flavin cofactor. Folate derivatives protect wild-type and mutant *E. coli* enzymes against flavin loss, and protect human MTHFR and the A222V mutant against thermal inactivation, suggesting a mechanism by which folate treatment reduces homocysteine levels.

Methylenetetrahydrofolate reductase (MTHFR) catalyzes the reduction of 5,10-methylenetetrahydrofolate (CH_2-H_4 folate) to 5-methyltetrahydrofolate (CH_3-H_4 folate), as shown in Equation (1).

$$CH_2\text{-}H_4 \text{ folate} + NAD(P)H \rightarrow CH_3\text{-}H_4 \text{ folate} + NAD(P)^+ \quad (1)$$

A noncovalently bound flavin adenine dinucleotide (FAD) cofactor accepts reducing equivalents from NAD(P)H and transfers them to CH_2-H_4 folate. Reduction of CH_2-H_4 folate by MTHFR is the only route for synthesis of the CH_3-H_4 folate that is utilized by methionine synthase to convert homocysteine to methionine.

Deficiency of MTHFR is the most common inborn error of folate metabolism and is a major genetic cause of hyperhomocysteinemia. One polymorphism, A222V (base change 677C→T), for which ~10% of the population is homozygous,[1, 2, 3, 4] is associated with mildly elevated fasting plasma homocysteine levels, especially in patients with low folate levels[5, 6, 7], and with reduced specific activity and increased thermolability of MTHFR in lymphocyte extracts.[1, 8] Homozygosity for the 677C→T mutation is the most common genetic cause of mildly elevated plasma homocysteine[7, 9] and is a risk factor for the development of cardiovascular disease.[1, 2, 3] The *T/T* genotype in either the mother or the fetus is also a risk factor for fetal neural tube defects.[10] Folic acid treatment decreases homocysteine levels[11] and dramatically reduces the incidence of neural tube defects.[12] The molecular bases for the impairment engendered by the 677C→T mutation and for the beneficial effects of folate are addressed here.

Human and other eukaryotic MTHFRs are dimeric enzymes composed of subunits of M_r 70,000–77,000. Determinants for binding of FAD, NAD(P)H and CH_2-H_4 folate are located in the N-terminal, M_r 40,000 portion; the C-terminal domain regulates enzyme activity in response to the demand for adenosylmethionine (AdoMet) and contains the binding site for this allosteric inhibitor. The subunits of MTHFRs of enteric bacteria are shorter chains ~300 residues in length. Their sequences can be aligned with the N-terminal catalytic domains of the eukaryotic MTHFRs[13], with 30% identity between the human and *E. coli* sequences (Figure 1). This level of primary sequence conservation predicts that the catalytic domains of the human and *E. coli* enzymes will possess similar structures.[14]

Many of the clinically significant mutations found so far in human MTHFR,[1, 13, 15, 16] including A222V, affect conserved residues in the catalytic domain. Human MTHFR has not yet been expressed at high enough levels to permit purification and biochemical investigation, so to investigate the molecular basis for impaired function in mutant human MTHFRs we have undertaken analyses of the enzyme from *E. coli*. The A222V mutation has been mimicked by constructing the corresponding A177V mutation in *E. coli*, and we have compared the biochemical properties of the bacterial wild-type and A177V mutant MTHFR proteins. The X-ray structure of the wild-type MTHFR from *E. coli* , reported here, provides a framework to relate genotypes to molecular phenotypes.

The structure of MTHFR

The structure of MTHFR, the first example of a $\beta_8\alpha_8$ barrel that binds FAD (Figure 2), has been solved using multiwavelength anomalous diffraction (Table 1). The chain tracing

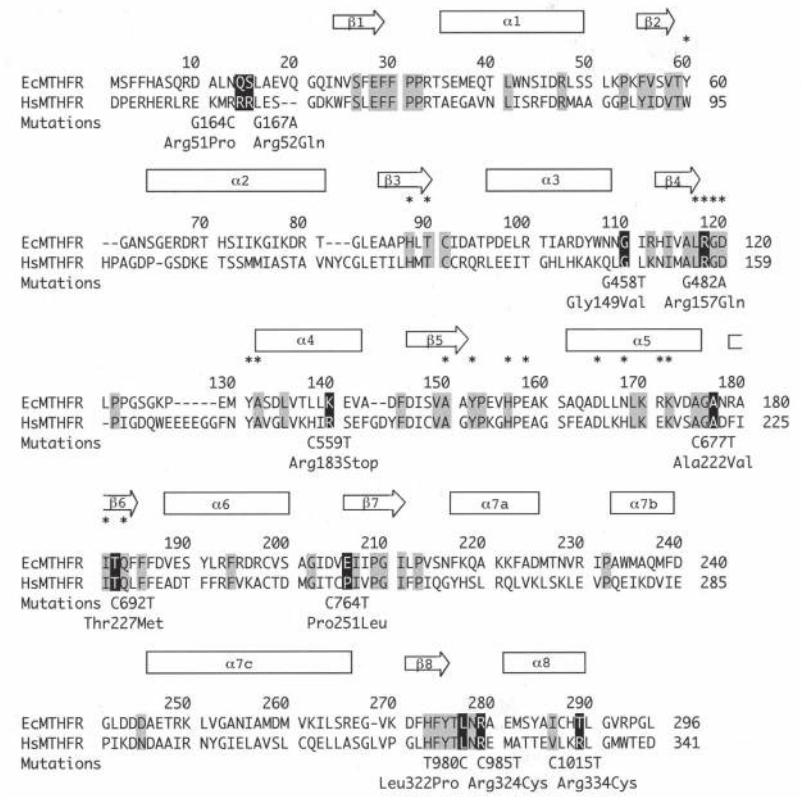

Figure 1. Alignment of the sequences of *E.coli* and human MTHFRs, based on simultaneous alignment of 12 MTHFR sequences and the positions of secondary structures in the *E.coli* enzyme. The locations of helices and β-strands in the structure are indicated by cylinders and arrows; residues flagged with asterisks interact with FAD in *E. coli* MTHFR. Shaded residues are identical in at least 9 of the 12 aligned MTHFR sequences. Sites of known mutations in the human enzyme are designated by black backgrounds, and the corresponding amino acid and nucleotide changes are shown. The N-terminal methionine is removed from the mature enzyme.

(Figure 2*c*) includes 273 residues; 20 N-terminal and two C-terminal residues are not visible in any of the three chains that compose the asymmetric unit. As expected for enzymes that form β/α barrels, the cofactor is bound at the C-termini of the β-strands. The flavin ring lies within the barrel with its plane parallel to the staves of the barrel and its *si* face exposed to solvent. The ribityl side chain and phosphate moieties are inserted between barrel strands 4 and 5, the ribosyl group adjoins helix 5, and the adenosyl group extends over the rim of the barrel.

Other known flavoenzymes that adopt β/α barrel folds bind flavin mononucleotide (FMN) rather than FAD. These enzymes — glycolate oxidase,[17] flavocytochrome b_2 (18), old yellow enzyme,[19] trimethylamine dehydrogenase,[20] and dihydroorotate dehydrogenase[21] — catalyze a variety of reactions, but FMN is bound in a similar fashion in all of them. Comparison of MTHFR with these enzymes shows that MTHFR breaks most of the structural rules that seemed to be established from the barrels that bind FMN. In the FMN-binding barrels, the ribityl phosphate side chain is inserted between strands 7 and 8, and the FMN phosphates are hydrogen-bonded to amides in the initial turn of a short but conserved helix, α8′, that precedes the α8-helix of the barrel. In MTHFR the ribityl side chain extends between barrel strands 4 and 5; there is no equivalent to the α8′ helix that binds the FMN phosphates, and the flavin ring is tilted by ~80° from its orientation in the other $\beta_8\alpha_8$ flavoenzymes. The novel aspects of FAD binding in the MTHFR $\beta_8\alpha_8$ barrel make it difficult to argue for divergent evolution of a flavin-binding family of barrel enzymes.

From the side view (Figure 2*b*), it is evident that strand 8 and helix 8 are both truncated relative to the rest of the β/α elements of the barrel. This truncation opens a groove running from the outer edge of the barrel to the accessible *si* face of the flavin. The pyridine nucleotide and folate substrates, NADH and CH_2-H_4 folate, are each expected to bind with the nicotinamide or pterin rings stacked over the open face of the isoalloxazine ring of the FAD to facilitate hydride transfer. Hydride transfer between the substrates and the flavin N(5) is known to occur at the *si* face of the flavin ring[22]. Model building suggests that the *p*-aminobenzoyl-glutamate moiety of methylenetetrahydrofolate lies in the groove. Thus the unusual truncation of the barrel elements β8 and α8 may be associated with the requirement to bind and react with the folate substrate.

The FAD-binding site

Electron density corresponding to the flavin ring and its protein environment has been calculated (Figure 3*a*), and the interactions of bound FAD with some of the conserved residues that form the binding site are depicted in a stereo drawing (Figure 3*b*). The residues that bind FAD are clustered at the ends of barrel strands β3, β4, and β5 and along helix α5 (Figs 1, 3*b*). The composition and spacing of these MTHFR sequences do not correspond to the characteristic sequence fingerprints associated with binding of flavin nucleotides[19, 23]. The backbone of FAD is crimped by a kink that buries the pyrophosphate and brings the C5 atoms of the ribityl and ribose groups into van der Waals contact. In contrast to many other flavoenzymes, MTHFR does not bind the flavin phosphate at the initial turn of an α-helix.

An intriguing feature of the FAD-binding site is the belt of side chains arching over the ribityl and phosphate groups and secured by the Arg 118−Glu 158 interaction that acts as a buckle (Figure 3*b*). The position of these residues suggests a role for the belt in the thermodynamics and kinetics of FAD binding. The β5-α5 connector, which includes Glu 158 from the belt buckle, encloses the ribityl-diphosphate-ribose segments of the FAD, so rearrangements of the protein must occur to let FAD enter or leave its binding site. One of the severe mutations in human MTHFR, R157Q (base change 482G→A) (13), alters the belt residue corresponding to Arg 118 in *E. coli* MTHFR. The role of Arg 118 in the structure of *E. coli* MTHFR strongly suggests that the R157Q mutant is defective in flavin binding.

Characterization of A177V mutant bacterial MTHFR.

The clinically significant A222V polymorphism in human MTHFR has been mimicked in the *E. coli* enzyme by introducing the homologous mutation A177V. When the catalytic properties of the wild-type and A177V mutant enzymes were compared, the mutation was found not to affect k_{cat} or the K_m values for CH_2-H_4 folate or NADH. The kinetic parameters of the wild-type enzyme were determined at 15 °C and pH 7.2 in a stopped-flow spectrophotometer[24]: K_m for NADH is 17 μM, K_m for CH_2-H_4 folate is 3.9 μM, and k_{cat} is 1,410 mol NADH oxidized min^{-1} (mol enzyme-bound FAD)$^{-1}$. The A177V mutation does not significantly change the measured kinetic parameters of MTHFR: K_m for NADH is 17 μM, K_m for CH_2-H_4 folate is 3.9 μM, and k_{cat} is 1,180 min^{-1}.

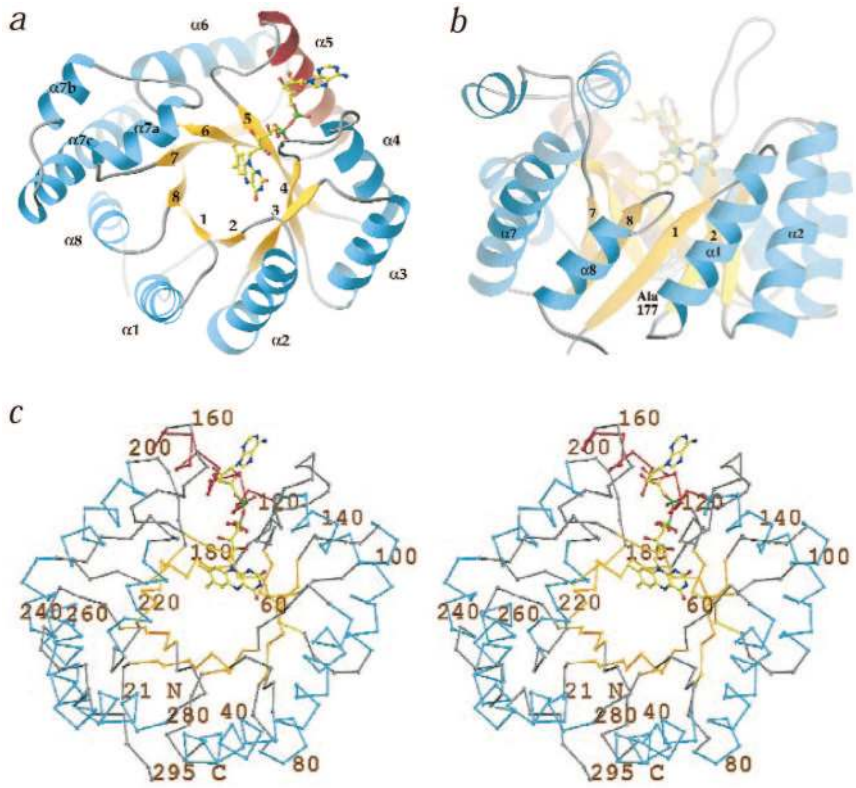

Figure 2. The structure of *E. coli* MTHFR. a) A view along the axis of the $\beta_8\alpha_8$ barrel looking toward the C-terminal ends of the β–strands[37]. FAD is drawn in ball-and-stick mode. Helix α5, which precedes the site corresponding to the human A→V polymorphism, is colored red in this and succeeding figures. **b)** A view perpendicular to the barrel axis and toward the *si* face of the flavin ring, showing the truncation of strand β8 and helix α8 and the resulting groove in which methylenetetrahydrofolate is expected to bind. Ala 177, the site of the Ala→Val mutation, is drawn with gray dot surfaces, and is at the rear of the barrel. **c)** A stereo drawing of the chain fold from approximately the same perspective as in (*a*).

Studies of the human A222V polymorphism have suggested that the mutant protein is more thermolabile than the wild-type protein as assessed by measurements of residual activity after heating lymphocyte extracts for 5 min at 46 °C (25) and by similar measurements with recombinant mutant human enzyme expressed in *E. coli*.[1] We investigated whether the A177V mutation was associated with thermolability of the bacterial enzyme using differential scanning calorimetry. The T_m was 53.8 °C for 60 μM mutant enzyme and 60.9 °C for wild-type protein at the same concentration (Figure 4). Both wild-type and mutant enzymes denature at progressively lower temperatures as their concentrations are decreased. Concentration-dependent melting temperatures are expected for systems in which an oligomer denatures to form unfolded protomers[26].

Gel filtration was used to demonstrate that *E. coli* MTHFR is a tetrameric enzyme that dissociates to dimers rather than monomers on dilution. When wild-type or A177V enzymes were applied to a Superose 12 FPLC column at an initial concentration of 60 μM, the relative molecular masses determined from the elution volumes were 119,000 ±2,000 (3.5 ±0.1 subunits mol^{-1}) for the wild-type enzyme and 108,000 ±10,000 for the mutant. The flavin cofactor remained bound to the tetrameric enzymes during the gel filtration as indicated by the flavin absorbance at 450 nm. Dilution of wild-type or mutant enzymes resulted in dissociation to dimers and loss of flavin. Dissociation to dimers is consistent with the arrangement of subunits found in the crystal structure. When the enzymes were applied to the gel column at initial concentrations of 500 nM, the estimated relative molecular masses were 65,000 ±7,000 (1.9 ±0.2 subunits mol^{-1}) for wild-type enzyme and 59,000 ±4,000 for the mutant enzyme. The flavin was released and eluted later, as indicated by monitoring flavin fluorescence.

These observations prompted further investigation of FAD binding by the A177V mutant and wild-type enzymes. FAD bound to MTHFR is not fluorescent; dissociation of FAD was therefore followed by measuring the fluorescence associated with the appearance of free flavin. The initial rate of flavin loss from the mutant was ~11 times that seen with the wild-type enzyme (Figure 5*a*, inset). The final fluorescence after dilution of the mutant protein to 500 nM indicated that all the flavin had been released. The enzyme concentration at which 50% of the flavin dissociated was 1.3 μM for the wild-type enzyme and 5.9 μM for the mutant protein. These data imply that the A177V mutation decreases the affinity of the protein for FAD. In both mutant and wild-type enzymes the initial rate of FAD loss varies as the square root of the enzyme concentration after dilution, as indicated by the fit of the data to the solid lines (Figure 5*a*). This dependence would be expected if the dissociation of the tetramer into dimers precedes the release of flavin. We conclude that the A177V mutation in the *E. coli* enzyme shifts the overall equilibrium between holoenzyme tetramers and apoenzyme dimers toward the formation of apoenzyme dimers.

Because FAD is an essential reactant in the enzyme-catalyzed electron transfer from NADH to CH_2-H_4 folate, flavin dissociation is accompanied by loss of enzyme activity. Enzyme activity was monitored under the same conditions as those used for the fluorescence measurements (Figure 5*a*). The A177V protein lost activity at a rate 10 times that for the wild-type protein, and the half-time for activity loss was the same as the half-time for the increase in flavin fluorescence, within the precision of the measurements (data not shown).

Since folate is known to lower homocysteine levels in the plasma, and to protect against the development of neural tube defects, we examined the effects of added folates on the rate of flavin dissociation and loss of enzyme activity after dilution of reductase. Addition of CH_3-H_4 folate (monoglutamate) reduced the rate of flavin loss from both the wild-type and mutant enzymes in a concentration-dependent manner (Figure 5 *b*). The mutant enzyme requires much higher levels of folate to decrease the initial rates of flavin loss to the values found for wild-type. When activity rather than fluorescence was measured following dilution into a solution containing added folate derivatives, in an experiment similar to that just mentioned (Figure 5*b*), the rate of loss of activity was decreased (data not shown). For *E. coli* MTHFR equivalent concentrations of CH_3-H_4 folate triglutamate were more effective than the monoglutamate at reducing the rate of flavin loss, consistent with the known K_m values for polyglutamate substrates.[27] Protection was also observed using the inhibitor dihydrofolate

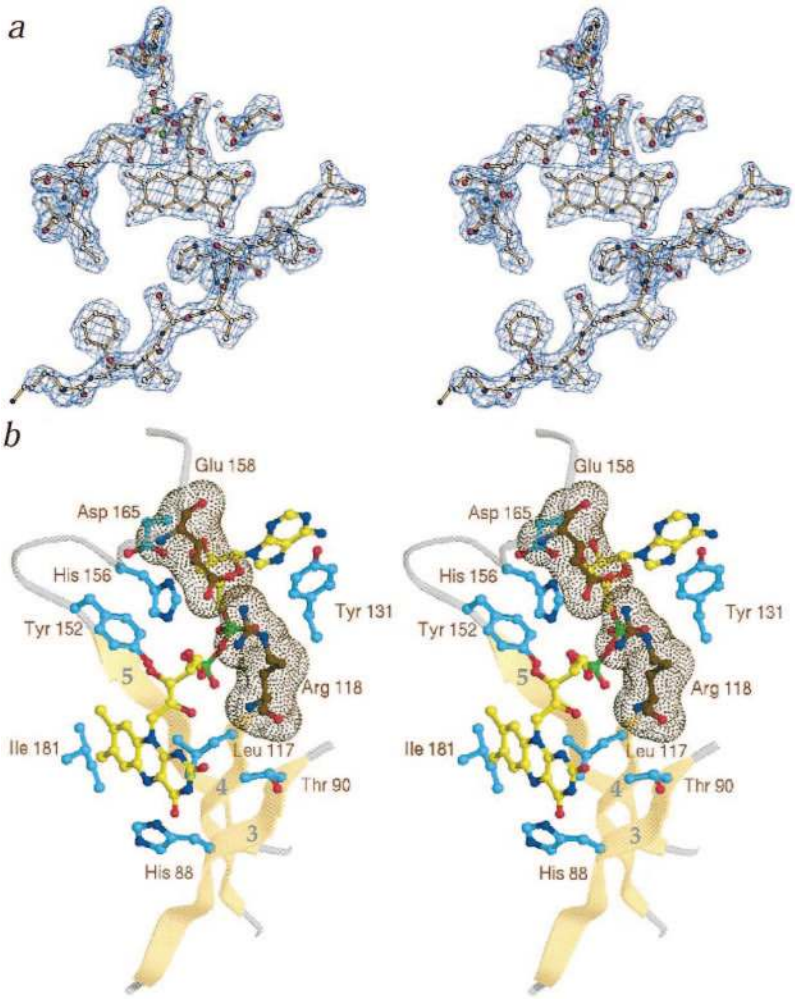

Figure 3. The FAD-binding site. a) The electron density in the vicinity of the cofactor, contoured at 1σ. The map was calculated with amplitudes ($2|F_o| - |F_c|$) and phases from the final refinement (Table 1); contours within 3 Å of model atoms are displayed. Residues surrounding the exposed *si* face are His 88, Asp 120, Thr 182 and Gln 183; β-strand 2 is in the foreground. **b)** A stereo drawing showing many of the conserved residues that contact bound FAD, which is drawn in ball-and-stick mode with atom coloring. Side-chain carbons are in cyan with oxygen and nitrogen atoms red and blue, respectively. The belt residues, Arg 118 and Glu 158, are distinguished by darker stick bonds and dot surfaces.

monoglutamate and the folate antagonist 5,10-dideazatetrahydrofolate pentaglutamate. We infer that any folate derivative that binds MTHFR slows the rate of dissociation of the flavin.

Mapping the A177V mutation onto the structure: the molecular phenotype

The A177V mutation affects FAD binding, but alters a residue that is not part of the FAD-binding site. In the *E. coli* enzyme, Ala 177 is located near the bottom of the $\beta_8\alpha_8$ barrel, out of direct contact with the flavin or with conserved residues that may be essential for activity or folate binding (Figs 2*b*, 6). This residue nestles in the loop connecting helix α5 with strand β6 and packs against atoms of Lys 172 in the preceding turn of the α5-helix, and against conserved residues Val 136 in helix α4 and Val 149 in strand β5. Mutating Ala 177 to valine is expected to perturb all of these packing interactions and to affect the secondary structures in which the neighbors of residue 177 reside. Propagation of packing changes to the FAD-binding site is easiest to envision as a perturbation of helix α5, which carries residues Lys 172, Asn 168, and Asp 165 that interact with the phosphate and ribosyl groups of the FAD (Figure 6*a*).

Interactions between chains of the tetrameric bacterial MTHFR may also be affected by the A177V mutation. The packing of chains in the tetramer of *E. coli* MTHFR is unusual (Figure 6*b*). The 12 monomers of the unit cell are arranged in layers in which either of two approximately planar arrangements of four chains can be selected as the tetramer that exists in solution. The tetramer we have designated has larger subunit–subunit contact areas, and polarities and compositions that are more characteristic for oligomer interfaces than for crystal packing contacts.[28, 29] The tetramer displays only C2 (two-fold) rather than the customary D2 (222) symmetry. The center of the tetramer is open, and the chains are held together by just two kinds of interfaces. The symmetry and packing of the subunits predict that the tetramers will dissociate to dimers, as observed in gel filtration of dilute enzyme solutions. The area calculated for the B–C interface is 800 $Å^2$, while that for the A–B interface is 500 $Å^2$; this suggests that the tetramer will dissociate into identical A-A′ and B-C dimers, across the interface that incorporates helix α5. Thus if steric overlap of Val 177 with its neighbors triggers movement of helix α5, the interactions across this interface will be affected.

Implications

Our comparison of the phenotypes of wild-type and A177V mutant MTHFR enzymes from *E. coli* suggests that the mutation leads to a thermolabile enzyme that loses its flavin cofactor more readily than does the wild type. This mutation accentuates properties inherent in the wild-type enzyme. With both wild-type and mutant enzymes, addition of folate derivatives results in decreased rates of flavin release and activity loss. We envision that protection by folate results from the increased affinity of MTHFR for FAD in the ternary complexes of enzyme, folate, and FAD.

The structure/function studies of the bacterial enzyme reported here provide a model for the role of folic acid in ameliorating hyperhomocysteinemia in humans, especially those homozygous for the A222V mutation. Although the human enzyme has not been fully characterized biochemically, our experiments (Figure 7) indicate that addition of methyltetrahydrofolate or FAD protects the human wild-type and mutant enzymes against thermal inactivation. The upper panel shows the protective effect of these compounds in crude extracts containing recombinant human enzyme expressed in *E. coli*[1], while in the lower panel lymphocyte extracts from Ala/Ala (normal MTHFR) or Val/Val (mutant MTHFR) human subjects have been used. Addition of FAD to crude extracts protects both wild-type and mutant enzymes, and the protection is more dramatic with the mutant enzyme. Addition of methyltetrahydrofolate to the crude extracts also protects both the wild-type and mutant enzymes against thermal denaturation, with the more dramatic protection again being seen with the mutant enzyme. *In vivo*, increased concentrations of folate derivatives that are products or inhibitors of the reaction will inhibit the reduction of CH_2-H_4 folate as well as stabilizing the enzyme. However, we assume that supplementation with folic acid increases the concentration of all intracellular

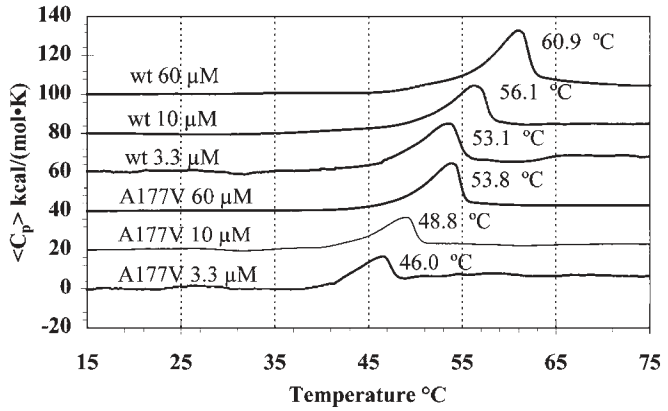

Figure 4. The A177V mutation leads to a thermolabile enzyme as assessed by differential-scanning calorimetry. Measurements were performed on wild-type and A177V MTHFR proteins at the indicated subunit concentrations. Each data set has been offset by 20 kcal mol^{-1} K^{-1} for clarity, and the melting temperatures (T_m) are displayed alongside their respective peaks. A preliminary experiment in which the T_m values of 22 µM wild-type and wild-type histidine-tagged MTHFR proteins were compared gave values of 58.4 and 58.6 °C, respectively, indicating that the His_6 tag at the C-terminus did not affect the melting temperature.

folate derivatives, including the substrate CH_2-H_4 folate. The results reported here suggest that increased folate, known to lower homocysteine levels in normal subjects[11] and in A→V homozygotes,[6] acts by suppressing loss of FAD from MTHFR.

Recent studies have demonstrated that folate deficiency in humans leads to uracil misincorporation into DNA and chromosome breakage, and have suggested that the 677C→T polymorphism might provide protection against chromosome breakage when the concentration of intracellular folates is low by sequestering folate in the CH_2-H_4 folate form that is required for conversion of dUMP to dTMP.[30] If the level of methylenetetrahydrofolate is low and MTHFR is fully active, flux will favor methionine biosynthesis over synthesis of thymidylate. Our studies suggest that wild-type MTHFR responds to low folate levels by undergoing flavin loss and inactivation. Our observations on bacterial and human MTHFR provide a biochemical rationale for the effects of folate supplements in reducing plasma homocysteine levels in individuals homozygous for the polymorphism. In addition, since folate derivatives stabilize both the wild-type and mutant enzymes, the benefit of folate supplementation should extend to individuals who are not homozygous for the polymorphism. Recent clinical studies suggest that individuals who are homozygous for the polymorphism might be particularly sensitive to homocysteine lowering by folate, although nonmutant individuals do respond.[31] Our results suggest that the activity of both wild-type and mutant enzymes may be controlled by the intracellular folate and FAD concentrations, and that the 677C→T mutation simply shifts the balance point at which enzyme inactivation occurs.

Methods

Overexpression and purification of wild-type and A177V mutant MTHFR.

Wild-type MTHFR was purified to homogeneity from *E. coli* strain CAS-9 as described.[24] Briefly, the coding sequence was placed into the polylinker region of plasmid p*Trc*99A (Pharmacia) and transformed into *metF* strain AB1909, which lacks a functional MTHFR and is auxotrophic for methionine, for overexpression. MTHFR was purified to homogeneity by batch chromatography on DEAE fast-flow Sepharose, FPLC on Mono Q anion-exchange resin, and hydrophobic FPLC on Phenyl Sepharose. This enzyme was used for structure determination. However, attempts to express the A177V protein in a similar manner led to very low levels of expression, and the protein was too unstable to survive the purification procedure. We therefore constructed strains expressing C-terminally histidine(6)-tagged wild-type[24] and A177V MTHFR. Plasmids containing the coding sequences for these proteins were used to transform *E. coli* strain BL21(DE3)*recD*$^+$ (Novagen). This strain contains a functional *metF* gene but only 1% of the MTHFR protein is wild-type and lacks the histidine tag. Histidine-tagged MTHFR from these strains could be purified to homogeneity in a single step

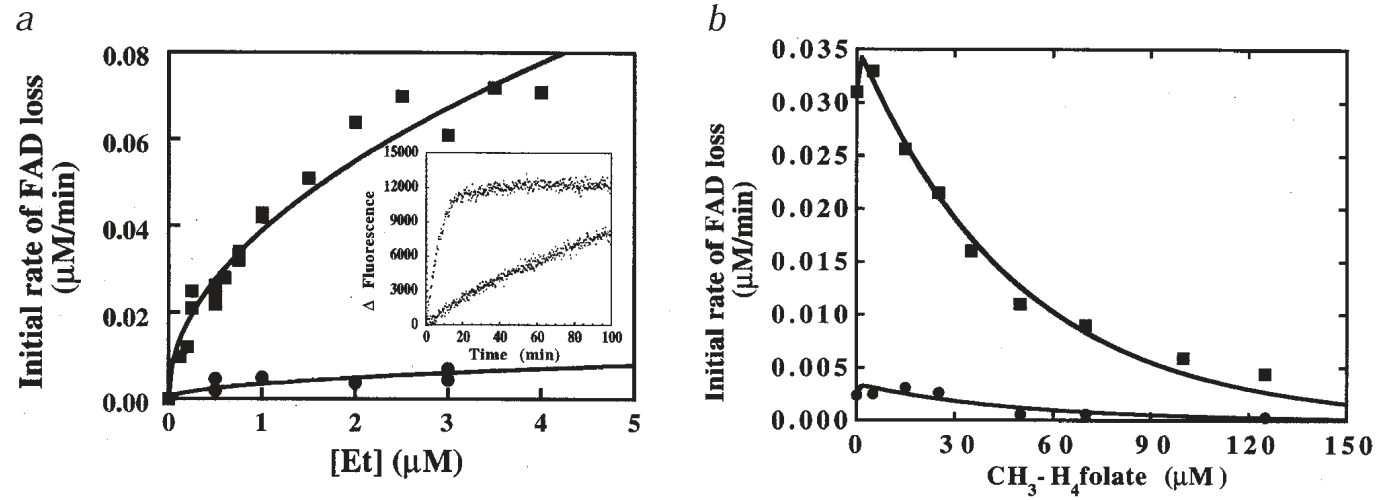

Figure 5. a) The A177V mutation is associated with an enhanced rate of flavin dissociation. After dilution of a concentrated stock of enzyme to the indicated subunit concentrations [Et], the initial rate of FAD dissociation was ascertained for wild-type (●) and A177V (■) enzymes. The solid lines have been calculated assuming that the rate of flavin release varies as the square root of the enzyme concentration after dilution. Inset: The change in fluorescence *versus* time is shown for wild-type (lower trace) and A177V (upper trace) enzymes diluted to 500 nM concentration. **b)** Protection of wild-type and A177V mutant enzyme against flavin loss after dilution in the presence of CH_3-H4 folate. The initial rate of flavin loss from 500 nM wild-type (●) and A177V mutant (■) enzymes is plotted against the concentration of (6*S*)CH_3-H_4 folate monoglutamate (Eprova Pharmaceuticals) present after dilution. The initial rates have been corrected for fluorescence increases associated with the slow oxidation of CH_3-H_4 folate catalyzed by the enzyme under aerobic conditions.

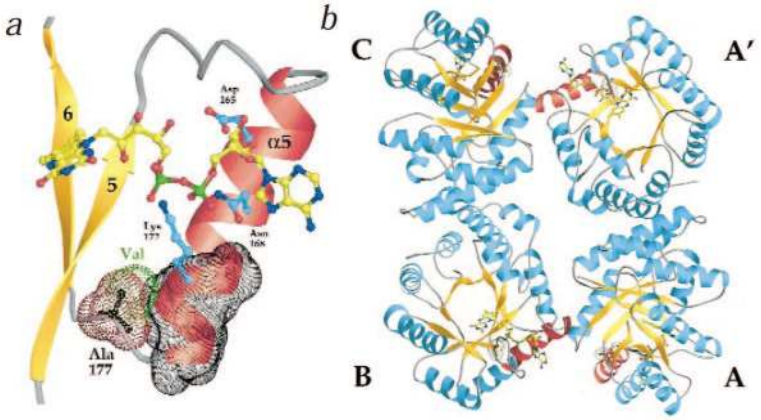

Figure 6. a) The location and environment of the Ala 177 that corresponds to the site of the A→V polymorphism in human MTHFR. The view is approximately perpendicular to the barrel axis and oriented to show helix α5 and its neighboring barrel strands. Black dot surfaces trace the helix backbone from 171 to 176; red surfaces represent the volume of alanine at position 177, and green surfaces a valine substituted at position 177 which clearly overlaps the helix backbone. The side chains of Lys 172, Asn 168, and Asp 165 that interact with FAD are drawn in ball-and-stick mode with carbons in cyan. **b)** The tetramer of *E. coli* MTHFR, viewed down the local two-fold axis. The asymmetric unit of the monoclinic cell contains the three chains A, B, and C; the fourth chain of the tetramer (A′) is related to A by a crystallographic two-fold axis. The C and B subunits can be superimposed on chains A and A′ by a local dyad (perpendicular to the page) that is inclined by ~53° to the crystallographic dyad along axis y. This local dyad is the only symmetry operator that relates the chains of the tetramer to one another. Interfaces A–A′ and B–C are formed by symmetric interactions between helices α7c, α7b, and α8. In contrast, the A and B (or C and A′) chains are not related by a simple rotation of $360/n^{O}$; the B chain is superimposed on the A chain by a rotation of 108° and a translation of ~7 Å. Helix 5, which may be critical in mediating the effects of mutation at position 177, is drawn in red, and Ala 177 is white and surrounded by dot surfaces. The figure was prepared using the program RIBBONS.[37]

by chromatography on Hi-Trap nickel agarose columns as described,[24] and yielded enzymes with a full complement of bound FAD (four per tetramer)[24] and with comparable specific activity as measured by CH_2-H_4 folate-menadione oxidoreductase assay.

Structure determination. The structure of *E. coli* MTHFR was determined by multiwavelength anomalous diffraction[32] (MAD) using mercury as the anomalous scatterer. Crystals suitable for data collection were obtained from 15% isopropanol, 100 mM MES pH 6.1, 40 μM FAD, 160 mM ammonium sulfate, and 8–13% polyethylene glycol (M_r 8,000) at 4 °C, and belong to space group C2 with unit cell dimensions a = 103.00 Å, b = 128.20 Å, c = 98.20 Å, and β = 121.60°, with three chains in the asymmetric unit. The MAD experiment (three wavelengths) was performed at CHESS beamline F2 with a crystal soaked in mercuric acetate and flash frozen. The CCP4 suite of programs[33] was used to locate the mercury sites by Patterson methods. Phases were calculated using the MAD option of MLPHARE[33] (<m> = 0.44–2.9 Å), and solvent flattening was performed with DM[33]. The model building for the three chains in the asymmetric unit was done in O.[34] X-PLOR[35] was used for refinement of the model in rounds that included simulated annealing and refinement of individual atom B-factors. A bulk solvent correction was applied.[36]

Differential-scanning calorimetry. Differential-scanning calorimetry was performed by Craig Johnson of Calorimetry Sciences Corporation on a NANO differential-scanning calorimeter. The excess heat capacity $<C_p>$ for thermal denaturation of purified enzyme in 50 mM potassium phosphate buffer, pH 6.3, containing 0.3 mM EDTA and 10% glycerol was measured for the indicated concentrations of wild-type and A177V histidine-tagged proteins over a temperature range from 15 to 75 °C. The temperature was increased at 1 °C min^{-1}.

Fluorimetry. Concentrated enzyme (~200 mM) was diluted to concentrations between 0.25 and 7 μM and the increase in fluorescence, a measure of FAD dissociation, was monitored over time. Fluorescence was measured with excitation at 390 nm and emission at 525 nm in an ISA JY/SPEX fluorimeter.

Coordinates. The coordinates have been deposited in the Protein Data Bank (accession code 1B5T).

Acknowledgments — We thank J. Shih (Lilly Corporation) for the gift of the pentaglutamate form of 5,10-dideazatetrahydrofolate. We are indebted to C. Johnson (Calorimetry Sciences), for performing the differential-scanning calorimetry experiments shown in Figure 4. We also thank A. Gafni for allowing us to use his fluorimeter and D. Ballou and V. Massey for assistance with the stopped-flow experiments. This work was supported by National Institute of General Medical Sciences grants to R.M and M.L., by NIH postdoctoral (B.G.) and predoctoral (C.S.) fellowships, by an NIH Cellular & Molecular Biology Training Grant (C.S.), and the Medical Research Council of Canada (R.R.) and by the McGill University Mary Louise Taylor predoctoral fellowship (P.T.).

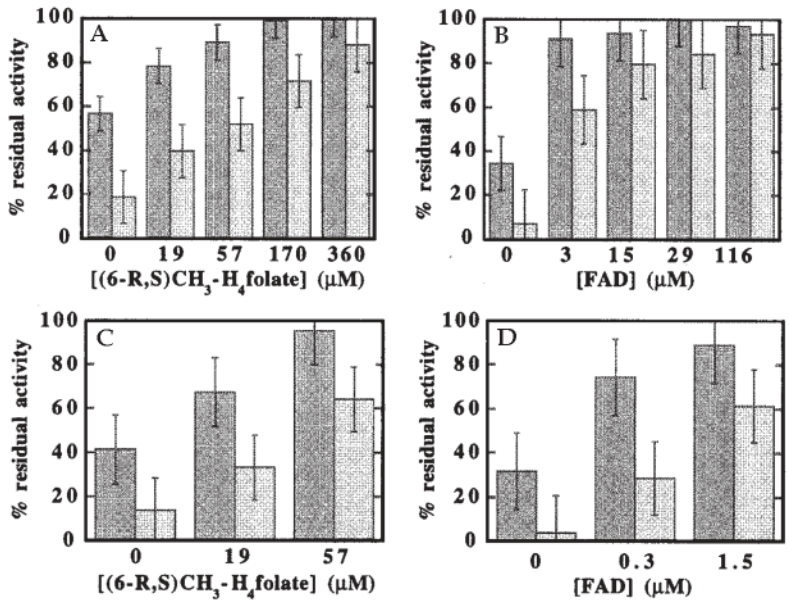

Figure 7. Stabilization of normal and mutant human MTHFR (hMTHFR) by CH_3-H_4 folate and FAD against heat inactivation. In each panel, the dark-gray columns represent data obtained for normal (Ala) MTHFR, while the light-gray stippled columns represent data obtained for mutant (Val) MTHFR. **a,b)** Stabilization of recombinant wild-type and A222V MTHFR expressed in *E. coli*[1]. Aliquots of crude sonicate supernatants containing 100 μg protein were preincubated at 46 °C in the presence of the indicated concentrations of (6-*RS*)CH_3-H_4 folate (*a*) or FAD (*b*). After cooling to 37 °C, additional (6-*RS*)CH_3-H_4 folate and/or FAD were added to the reaction mixtures and the samples were assayed in duplicate using the CH_3-H_4 folate-menadione oxidoreductase assay[1, 38]. Values reported have been corrected for the activity in a control JM105 strain[1]. The bars represent the mean ±s.d. of data obtained from three experiments. **c**, **d)** Stabilization of normal (Ala/Ala) and mutant (Val/Val) MTHFR in human lymphocyte extracts (90 μg of protein) by CH_3-H_4 folate (*c*) and FAD (*d*). The bars represent the mean ±s.d. of data obtained from duplicate assays of the enzyme extracts of three individuals.

Table 1. X-ray data collection, MAD phasing, and structure refinement

Data collection

Crystal	Wavelength (Å)	Resolution (Å)	Completeness (%)	No. of observations	Unique reflections	R_{sym}[1]
λ1	1.012	2.5	97.3 (81.4)	375,635	36,377	0.060 (0.091)
λ2	1.010	2.5	97.2 (80.4)	376,949	36,492	0.066 (0.097)
λ3	1.008	2.5	97.3 (83.0)	377,615	36,508	0.068 (0.101)

MAD phasing

Resolution (Å)[2]	13.64	8.92	6.63	5.27	4.38	3.74	3.27	2.90
<m>	0.462	0.423	0.499	0.513	0.454	0.412	0.434	0.435

Statistics after refinement

Resolution (Å)	20.0–2.5	R_{work}	0.212
Reflections[3]	36,486	R_{free}	0.263
Protein + FAD atoms	6,378	Deviations in	
Solvents	184	Bond length	0.008 Å
Average B (protein)	21.36 Å^2	Bond angles	1.4°
Average B (solvents)	26.20 Å^2	Improper dihedrals	1.2°

1. Values in parentheses are for outermost bins.
2. High-resolution limit for bins.
3. No σ cutoff.

References

1. Frosst, P. *et al.* A candidate genetic risk factor for vascular disease: a common mutation in methylenetetrahydrofolate reductase. *Nature Genet.* **10**, 111–113 (1995).
2. Kluijtmans, L.A. *et al.* Molecular genetic analysis in mild hyperhomocysteinemia: a common mutation in the methylenetetrahydrofolate reductase gene is a genetic risk factor for cardiovascular disease. *Am. J. Hum. Genet.* **58**, 35–41 (1996).
3. Morita, H. *et al.* Genetic polymorphism of 5,10-methylenetetrahydrofolate reductase (MTHFR) as a risk factor for coronary artery disease. *Circulation* **95**, 2032–2036 (1997).
4. Wilcken, D.E., Wang, X.L., Sim, A.S. & McCredie, R.M. Distribution in healthy and coronary populations of the methylenetetrahydrofolate reductase (MTHFR) C677T mutation. *Arteroscler. Thromb. Vasc. Biol.* **16**, 878–882 (1996).
5. Ma, J. *et al.* Methylenetetrahydrofolate reductase polymorphism, plasma folate, homocysteine, and risk of myocardial infarction in US physicians. *Circulation* **94**, 2410–2416 (1996).
6. Jacques, P.F. *et al.* Relation between folate status, a common mutation in methylenetetrahydrofolate reductase, and plasma homocysteine concentrations. *Circulation* **93**, 7–9 (1996).
7. Harmon, D.L. *et al.* The common "thermolabile" variant of methylenetetrahydrofolate reductase is a major determinant of mild hyperhomocysteinaemia. *Q. J. Med.* **89**, 515–577 (1996).
8. van der Put, N. *et al.* Mutated methylenetetrahydrofolate reductase as a risk factor for spina bifida. *Lancet* **346**, 1070–1071 (1995).
9. Refsum, H., Ueland, P.M., Nygard, O. & Vollset, S. Homocysteine and cardiovascular disease. *Annu. Rev. Med.* **49**, 31–62 (1998).
10. van der Put, N.M.J., Eskes, T.K.A.B. & Blom, H.J. Is the common 677C →T mutation in the methylenetetrahydrofolate reductase gene a risk factor for neural tube defects? A meta-analysis. *Q. J. Med.* **90**, 111–115 (1997).
11. Boushey, C.J., Beresford, S.A.A., Omenn, G.S. & Motulsky, A.G. A quantitative assessment of plasma homocysteine as a risk factor for vascular disease. *JAMA* **274**, 1049–1057 (1995).
12. Vitamin Study Research Group, M.R.C. Prevention of neural-tube defects. *Lancet* **338**, 131–137 (1991).
13. Goyette, P. *et al.* Human methylenetetrahydrofolate reductase: isolation of cDNA, mapping and mutation identification. *Nature Genet.* **7**, 195–200 (1994).
14. Sander, C. & Schneider, R. Database of homology-derived protein structures and the structural meaning of sequence alignment. *Proteins* **9**, 56–68 (1991).
15. Goyette, P., Christensen, B., Rosenblatt, D.S. & Rozen, R. Severe and mild mutations in cis for the methylenetetrahydofolate reductase (MTHFR) gene, and description of five novel mutations in MTHFR. *Am. J. Hum. Genet.* **59**, 1268–1275 (1996).
16. Goyette, P., Frosst, P., Rosenblatt, D.S. & Rozen, R. Seven novel mutations in the methylenetetrahydrofolate reductase gene and genotype/phenotype correlations in severe methylenetetrahydrofolate reductase deficiency. *Am. J. Hum. Genet.* **56**, 1052–1059 (1995).
17. Lindqvist, Y. Refined structure of spinach glycolate oxidase at 2 Å resolution. *J. Mol. Biol.* **209**, 151–166 (1989).
18. Xia, Z.X. & Mathews, F.S. Molecular structure of flavocytochrome b_2 at 2.4 Å resolution. *J. Mol. Biol.* **212**, 837–863 (1990).
19. Fox, K.M. & Karplus, P.A. Old yellow enzyme at 2 Å resolution: overall structure, ligand binding, and comparison with related flavoproteins. *Structure* **2**, 1089–1105 (1994).
20. Lim, L.W. Three-dimensional structure of the iron-sulfur flavoprotein trimethylamine dehydrogenase at 2.4 Å resolution. *J. Biol. Chem.* **261**, 15140–15146 (1986).
21. Rowland, P., Nielsen, F.S., Jensen, K.F. & Larsen, S. The crystal structure of the flavin containing enzyme dihydroorotate dehydrogenase A from *Lactococcus lactis*. *Structure* **5**, 239–252 (1997).
22. Sumner, J.S. & Matthews, R.G. Stereochemistry and mechanism of hydrogen transfer between NADPH and methylenetetrahydrofolate in the reaction catalyzed by methylenetetrahydrofolate reductase from pig liver. *J. Am. Chem. Soc.* **114**, 6949–6956 (1992).
23. Eggink, G., Engel, H., Vriend, G., Terpstra, P. & Witholt, B. Rubredoxin reductase of *Pseudomonas oleovorans.* Structural relationship to other flavoprotein oxidoreductases based on one NAD and two FAD fingerprints. *J. Mol. Biol.* **212**, 135–142 (1990).
24. Sheppard, C.A., Trimmer, E.E. & Matthews, R.G. Purification and properties of NADH-dependent 5,10-methylenetetrahydrofolate reductase from *Escherichia coli*. *J. Bacteriol.* **181**, 718–725 (1999).
25. Kang, S.-S. *et al.* Thermolabile methylenetetrahydrofolate reductase: an inherited risk factor for coronary artery disease. *Am. J. Hum. Genet.* **48**, 536–545 (1991).
26. Li, W.-T. *et al.* Thermodynamic stability of arachaeal histones. *Biochemistry* **37**, 10563–10572 (1998).
27. Matthews, R.G. & Baugh, C.M. Interactions of pig liver methylenetetrahydrofolate reductase with methylenetetrahydropteroylpolyglutamate substrates and with dihydropteroylpolyglutamate inhibitors. *Biochemistry* **19**, 2040–2045 (1980).
28. Jones, S. & Thornton, J.M. Protein–protein interactions: a review of protein dimer structures. *Prog. Biophys. Mol. Biol.* **63**, 31–65 (1995).
29. Lijnzaad, P. & Argos, P. Hydrophobic patches on protein subunit interfaces: characteristics and prediction. *Proteins* **28**, 333–343 (1997).
30. Blount, B.C. *et al.* Folate deficiency causes uracil misincorporation into human DNA and chromosome breakage: implications for cancer and neuronal damage. *Proc. Natl. Acad. Sci. USA* **94**, 3290–3295 (1997).
31. Deloughery, T.G. *et al.* Common mutation in methylenetetrahydrofolate reductase. Correlation with homocysteine metabolism and late-onset vascular disease. *Circulation* **94**, 3074–3078 (1996).
32. Hendrickson, W.A. & Ogata, C.M. Phase determination from multiwavelength anomalous diffraction experiments. *Methods Enzymol* **276**, 494–522 (1997).
33. The CCP4 suite: programs for protein crystallography.*Acta Crystallogr. D* **50**, 760–763 (1994).
34. Jones, T.A. & Kjeldgaard, M. *O—The manual*, (Uppsala University, Uppsala; 1993).
35. Brünger, A.T. *X-PLOR: a system for X-ray crystallography and NMR* (Yale University Press, New Haven, CT; 1992).
36. Jiang, J.S. & Brünger, A.T. Protein hydration observed by X-ray diffraction. Solvation properties of penicillopepsin and neuraminidase crystal structures. *J. Mol. Biol.* **264**, 100–115 (1994).
37. Carson, M. Ribbons. *Methods Enzymol.* **277**, 493–504 (1997).
38. Rosenblatt, D.S. & Erbe, R.W. Methylenetetrahydrofolate reductase in cultured human cells. I. Growth and metabolic studies. *Pediatr. Res.* **11**, 1137–1141 (1977).